Bloodstream form *Trypanosoma brucei* depend upon multiple metacaspases associated with RAB11-positive endosomes

Matthew J. Helms[1],[*], Audrey Ambit[1],[*], Paul Appleton[2], Laurence Tetley[2], Graham H. Coombs[2] and Jeremy C. Mottram[1],[‡]

[1]Wellcome Centre for Molecular Parasitology, The Anderson College, University of Glasgow, Glasgow G11 6NU, UK
[2]Division of Infection and Immunity, Institute of Biomedical and Life Sciences, Joseph Black Building, University of Glasgow, Glasgow G12 8QQ, UK

[*]These authors contributed equally to this work
[‡]Author for correspondence (e-mail: j.mottram@udcf.gla.ac.uk)

Summary

Trypanosoma brucei possesses five metacaspase genes. Of these, *MCA2* and *MCA3* are expressed only in the mammalian bloodstream form of the parasite, whereas *MCA5* is expressed also in the insect procyclic form. Triple RNAi analysis showed MCA2, MCA3 and MCA5 to be essential in the bloodstream form, with parasites accumulating pre-cytokinesis. Nevertheless, triple null mutants (Δ*mca2/3*Δ*mca5*) could be isolated after sequential gene deletion. Thereafter, Δ*mca2/3*Δ*mca5* mutants were found to grow well both in vitro in culture and in vivo in mice. We hypothesise that metacaspases are essential for bloodstream form parasites, but they have overlapping functions and their progressive loss can be compensated for by activation of alternative biochemical pathways. Analysis of Δ*mca2/3*Δ*mca5* revealed no greater or lesser susceptibility to stresses reported to initiate programmed cell death, such as treatment with prostaglandin D$_2$. The metacaspases were found to colocalise with RAB11, a marker for recycling endosomes. However, variant surface glycoprotein (VSG) recycling processes and the degradation of internalised anti-VSG antibody were found to occur similarly in wild type, Δ*mca2/3*Δ*mca5* and triple RNAi induced parasites. Thus, the data provide no support for the direct involvement of *T. brucei* metacaspases in programmed cell death and suggest that the proteins have a function associated with RAB11 vesicles that is independent of known recycling processes of RAB11-positive endosomes.

Supplementary material available online at
http://jcs.biologists.org/cgi/content/full/119/6/1105/DC1

Key words: Metacaspase, Endosomes, Recycling, *Trypanosoma*, Programmed cell death, RNAi

Introduction

Trypanosoma brucei is a unicellular parasitic protozoon responsible for sleeping sickness in humans and nagana in cattle in sub-Saharan Africa. This parasite has a digenetic life cycle, alternating between a mammalian host and the insect vector, the tsetse fly. In the mammalian bloodstream the parasite lives extracellularly, with the surface of the parasite being covered with a dense coat of variant surface glycoprotein (VSG) which is attached to the plasma membrane with a glycosylphosphatidylinositol (GPI) anchor (Ferguson, 1999). The differential expression of VSG genes allows the parasite to undergo antigenic variation and thus evade the host's immune response (Barry and McCulloch, 2001). The surface VSG undergoes rapid internalisation and recycling (Seyfang et al., 1990) via the flagellar pocket, which is the only site of endocytosis and exocytosis for the parasite. This recycling may function as a secondary defence against immune challenge, aiding in the removal of host anti-VSG antibodies (O'Beirne et al., 1998). The antibodies are internalised, degraded and then secreted (Jeffries et al., 2001; Pal et al., 2003), although the enzymes responsible for degradation are yet to be elucidated.

Cysteine peptidases belong to several clans that have separate evolutionary origins (Rawlings et al., 2004). Members of clan CA, containing lysosomal cysteine peptidases, are abundant in trypanosomes and other parasitic protozoa and are important virulence factors and drug targets (Klemba and Goldberg, 2002; Mottram et al., 2004). Metacaspases are clan CD cysteine peptidases that have been identified in plants, fungi and protozoa, but not in worms, flies or mammals (Uren et al., 2000). Metacaspases from plants have been classified into type-I and type-II (Uren et al., 2000) and have been proposed to be part of the developmental cell death machinery. They have been implicated in maintenance of the balance between death and proliferation required for plant embryogenesis (Suarez et al., 2004; Bozhkov et al., 2005). Evidence is also accumulating for a role in cell death of the *Saccharomyces cerevisiae* metacaspase YCA1 (Madeo et al., 2002; Herker et al., 2004; Bettiga et al., 2004; Wadskog et al., 2004; Madeo et al., 2004). Overexpression of YCA1 resulted in both fragmented DNA and chromatin condensation, and these features were abolished by co-incubation with the caspase inhibitor Z-VAD-fluoromethylketone (Madeo et al.,

2002). Moreover, deletion of *YCA1* appeared to hinder apoptosis. Thus, whereas yeast deleted for *SRO7* (the homologue of a *Drosophila* tumour suppressor gene) showed an increased sensitivity to NaCl stress (Wadskog et al., 2004) with a rapid loss in viability accompanied by markers of apoptosis, the additional deletion of *YCA1* reduced this fast initial drop in viability and the level of DNA fragmentation of the salt-stressed *SRO7*-deficient line. Similarly, the deletion of the yeast deubiquitylating enzyme UBP10 resulted in a complex phenotype characterised by a sub-population of cells displaying markers of apoptosis (Bettiga et al., 2004). The further deletion of *YCA1* suppressed this phenotype, whereas the overexpression of YCA1 resulted in an increased number of cells displaying apoptotic markers. Furthermore, metacaspase involvement in apoptotic-like cell death has also been reported for yeast with regard to chronological aging (Herker et al., 2004), mRNA stability (Mazzoni et al., 2005), defects in initiation of DNA replication (Weinberger et al., 2005) and in response to viral infection (Ivanovska and Hardwick, 2005).

It has been reported that the heterologous expression of a *T. brucei* metacaspase (*Tb*MCA4) in *S. cerevisiae* resulted in growth inhibition, mitochondrial dysfunction and cell death (Szallies et al., 2002). It has also been proposed that in trypanosomatids metacaspases function as caspase-like enzymes and are involved in apoptosis-like cell death, often called 'programmed cell death' (PCD) (Debrabant et al., 2003; Nguewa et al., 2004). PCD has been reported for a number of trypanosomatids, with there being evidence for cytoplasmic blebbing, DNA fragmentation, phosphoserine exposure, release of cytochrome *C* and changes in mitochondrial membrane potential (Ameisen, 1996; Ameisen et al., 1996; Welburn et al., 1996; Das et al., 2001; Zangger et al., 2002; Lee et al., 2002; Holzmuller et al., 2002; Arnoult et al., 2002a; Arnoult et al., 2002b; Sen et al., 2004; Figarella et al., 2005). However, to date there has been only one report of apoptosis-like cell death in bloodstream form (BSF) *T. brucei* (induced by prostaglandin D$_2$ (Figarella et al., 2005)), whereas PCD apparently resulted from treatment of procyclic form (PCF) *T. brucei* with the lectin concanavalin A (Welburn et al., 1996; Welburn and Murphy, 1998; Pearson et al., 2000) or reactive oxygen species (Ridgley et al., 1999). Nevertheless, definitive biochemical evidence to support PCD in trypanosomes is lacking and the trypanosome genome appears to lack vital components of two of the central effector pathways of mammalian apoptosis; caspases and their activation, and mitochondrial membrane permeabilization by BCL-2.

We tested the hypothesis that metacaspases in trypanosomatids are involved in PCD by investigating the expression, localisation and function of three *T. brucei* metacaspases: MCA2, MCA3 and MCA5. These three metacaspases have predicted active-site cysteine and histidine residues essential for cysteine peptidase activity, whereas the other two *T. brucei* metacaspases, MCA1 and MCA4, have substitutions in these residues and are predicted to lack cysteine peptidase activity (Mottram et al., 2003). The finding that MCA2 and MCA3 are stage-regulated, that the metacaspases do not undergo any caspase-like processing under normal growth conditions or after prostaglandin D$_2$ treatment to induce cell death, and that they are colocated in part in RAB11-positive vesicles argues against a caspase-like

involvement in PCD. Rather, the proteins would appear to have a function that is independent of RAB11-dependent recycling of VSG or transferrin receptor, and the degradation and secretion of anti-VSG IgG and transferrin. Loss of this function, which may involve cell-cycle control in Δ*mca2/3*Δ*mca5* mutants, has severe, although temporary, effects because adaptation – potentially through changes in cell signalling, allowing survival – had already been initiated during the sequential gene deletion and prolonged selection. However, simultaneous RNA silencing of *MCA2*, *MCA3* and *MCA5* leads to a very severe phenotype with an immediate growth arrest, indicating that these three metacaspases play crucial roles for the cell.

Results

Expression profile of MCA2, MCA3 and MCA5 in *T. brucei*

The *MCA2* and *MCA3* genes are located in a tandem repeat on chromosome 6 of *T. brucei* and the encoded proteins share 89% amino acid identity, diverging only in the N-terminal region where MCA3 has a small extension relative to MCA2 (Szallies et al., 2002; Mottram et al., 2003). MCA5 is unique among the *T. brucei* metacaspases in that it possesses a C-terminal extension relative to the others (Mottram et al., 2003). An alignment of MCA2, MCA3 and MCA5 (supplementary material Fig. S1) shows the positions of the predicted active site histidine and cysteine residues, together with putative class III WW binding domain motifs. WW binding domains act as ligands for WW domains, which are modules mediating protein-protein interactions in a diverse range of cellular processes (Sudol and Hunter, 2000). Class III WW binding domains are characterised by poly-proline motifs flanked by arginine or lysine residues (Macias et al., 2002). Motifs fulfilling these requirements were identified in the N-terminal regions of MCA2 and MCA3 and the C-terminal extension of MCA5 (supplementary material Fig. S1).

A rabbit polyclonal antibody was raised against a long peptide that, in MCA2 and MCA3, spans the central domain containing both the predicted catalytic cysteine and histidine residues (Fig. S1). Western blot analysis using this antibody on whole-cell lysates of *T. brucei* detected the 37 kDa MCA2 and the 39 kDa MCA3 in the BSF but not the PCF (Fig. 1A). The antibody also detected a major crossreacting protein of 48 kDa and a minor one of 37 kDa in both life-cycle stages, which act as internal controls for protein loading. A sheep polyclonal antibody raised against full-length recombinant MCA5 detected similar levels of expression of the 55 kDa MCA5 in PCF and BSF cell lysates (Fig. 1B). The finding that MCA2, MCA3 and MCA5 were each detected at a similar molecular mass to that predicted from the gene sequences indicates that in wild-type *T. brucei* no major processing of the metacaspases occurs under standard in vitro growth conditions.

Metacapase function analysed by RNAi

A gene fragment, identical in *MCA2* and *MCA3,* was cloned into the p2T7^{ti} RNAi vector and used to transfect a BSF RNAi cell line. Western blot analysis confirmed downregulation of MCA2 and MCA3 to undetectable levels in two independent clones (one shown in Fig. 2A) after induction with tetracycline for 24 hours (Fig. 2A, upper left panel), whereas the crossreacting protein of 48 kDa (marked *) and MCA5 levels

Fig. 1. Expression of metacaspases. (A,B) Total cell lysates were prepared from *T. brucei* PCF (lane 1) and BSF (lane 2). 5×10^6 cell equivalents were then subjected to SDS-PAGE and transferred to PVDF membrane prior to immunoblotting with immunopurified rabbit anti-MCA2-MCA3 antibodies (A) or with sheep anti-MCA5 antiserum (B). MCA2, MCA3 and MCA5 are indicated. A crossreacting 48 kDa protein (A, see *) and an antibody against EF-1α demonstrates equal loading. (C) Western blots prepared with BSF wild-type (lane 1) and transgenic parasites expressing an ectopic copy of either *MCA3HA* (lane 2) or *MCA2HA* (lane 3) were probed with a monoclonal anti-HA antibody. MCA2HA and MCA3HA are indicated at their predicted sizes of 40 and 41 kDa, respectively.
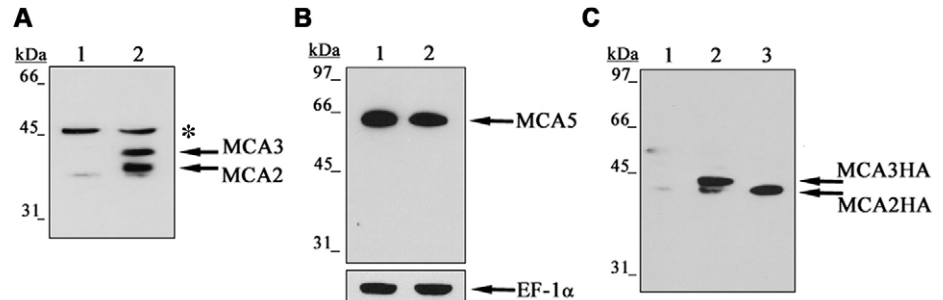
(lower left panel) remained the same before and after induction. RNAi was also performed with a construct targeted to MCA5 (Fig. 2A, right panel). In this case, in two independent clones, MCA5 expression was very greatly downregulated (Fig. 2A, upper right panel), whereas MCA2 and MCA3 levels remained the same before and after induction (lower right panel). The *MCA2* and *MCA3* RNAi clones and the *MCA5* RNAi clones grew at the same rate before and after induction. Since MCA2 and MCA3 expression could not be detected in PCF parasites (Fig. 1A), we carried out RNAi of just *MCA5* in PCF parasites. In two independent clones, MCA5 expression was reduced below the level of detection following induction with tetracycline (data not shown), but no growth phenotype was observed. This suggests that expression of MCA2, MCA3 and MCA5 is not required for PCF parasites in in vitro culture.

A further BSF cell line was generated for triple RNAi of *MCA2, MCA3* and *MCA5*. In two independent clones (one shown in Fig. 2B), a rapid growth arrest was observed following RNAi induction (Fig. 2B, upper panel). Western blot analysis confirmed almost total downregulation of MCA2, MCA3 and MCA5 after induction with tetracycline for 24 hours (Fig. 2B, lower panels), whereas the level of the crossreacting protein of 48 kDa (marked *) remained constant. Indeed MCA2 and MCA3 were not detectable by 4 hours (data not shown). Analysis of kinetoplast and nuclei configuration in induced cells was performed to analyse the progression of the parasites through the cell cycle in comparison to wild type (Fig. 2C). At 4 hours post-induction, a significant increase was observed in the number of cells with one nucleus and one kinetoplast (1N1K) (Fig. 2C lower panel). This increase was attributed to an accumulation of cells with a bone-shaped kinetoplast (41% of the 1N1K cells vs 27% in the non-induced, Fig. 2D, upper panel) indicating that kinetoplast segregation was impaired. The concomitant appearance of aberrant cells with two nuclei and a single big kinetoplast (2N1K, Fig. 2C), not normally found in wild-type cells because kinetoplast division typically occurs before mitosis, confirmed the delay in kinetoplast segregation. By 8 hours post-induction, many 1N1K cells had belatedly managed to divide their kinetoplast, leading to a slight increase of 1N2K cells (Fig. 2C). Most marked, however, was an accumulation of 2N2K cells, suggesting a post-mitotic block before the start of furrow ingression at cytokinesis. Cells appeared to be unable to escape this pre-cytokinesis block, because by 12 hours post-induction the number of cells

with multiple nuclei and kinetoplasts was almost four times higher than in the non-induced control, showing that DNA replication and mitosis still occurred but cell division invariably failed. These data suggest that MCA2, MCA3 and MCA5 expression is required for multiplication of BSF *T. brucei*, but that the proteins can individually compensate for the loss of each other.

MCA null mutants are viable in vitro and in vivo

Since the RNAi studies indicated that *T. brucei* BSF are viable when MCA5 or MCA2-MCA3 are expressed, BSF *MCA*-deficient cell lines were generated by sequential rounds of targeted gene replacement (Fig. 3A). The simultaneous deletion of *MCA2* and *MCA3* was achieved by selection of unique sequences flanking the locus. *BSD* and *PAC* resistance markers were used to replace the two alleles from BSF parasites, and two independent clonal lines (Δ*mca2/3*) were established. Correct integration of the drug-resistance cassettes and the deletion of *MCA2* and *MCA3* were confirmed by Southern blotting (Fig. 3B). Genomic DNA was digested with *Kpn*I and the Southern blot probed with the 3′ flanking region. Loss of the 8.8 kb DNA fragment containing the *MCA2-MCA3* locus in the null mutants correlated with the appearance of 1.9 and 1.7 kb DNA fragments representing the *PAC* and *BSD* cassettes (lanes 4 and 5). The loss of MCA2 and MCA3 protein was confirmed by western blotting (Fig. 3C). The two Δ*mca2/3* BSF clones were found to be viable in culture and showed no significant differences with regard to growth rate or gross morphology when compared with wild-type parasites. In addition, the Δ*mca2/3* clones were as virulent to mice as wild-type parasites and achieved a mean parasitaemia of 1×10^9 ml^{-1}, 4 days after inoculation of 1×10^3 cells.

To investigate in more detail the needs for individual MCAs and the possibility of redundancy within the MCA family, *MCA5* was deleted from both PCF and BSF parasites. Sequential rounds of targeted gene disruption were carried out with the antibiotic resistance genes for hygromycin and neomycin (*HYG* and *NEO*, respectively) as selectable markers. Δ*mca5* mutants were generated in both life-cycle stages and confirmed by PCR and western blotting (Fig. 3D and data not shown). Both BSF and PCF Δ*mca5* parasites displayed no discernible difference in either morphology or growth rate compared with wild-type parasites. The same *MCA5* deletion constructs were used in an attempt to generate BSF Δ*mca2/3*Δ*mca5* triple null mutants by sequential rounds of transfection into Δ*mca2/3* clone 1. In light
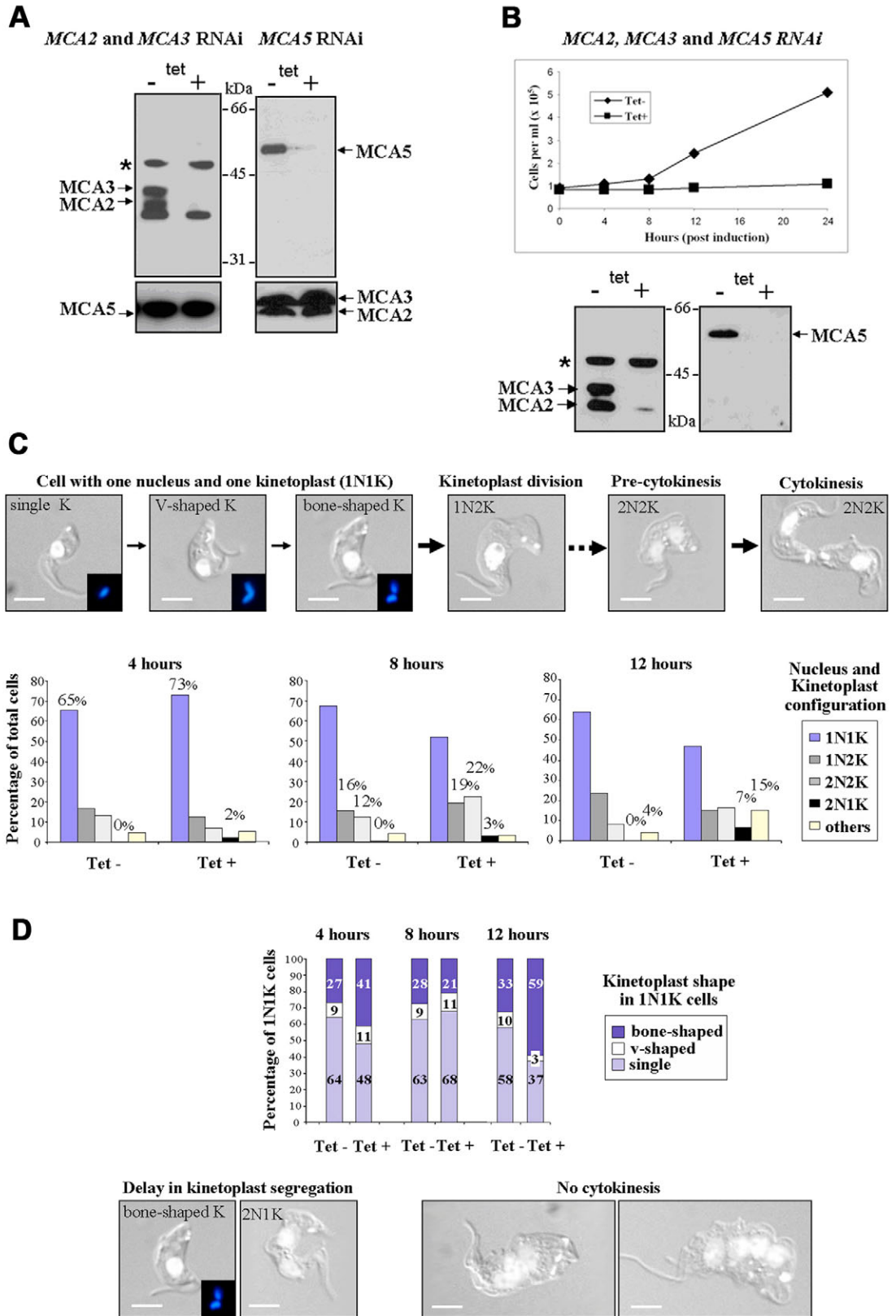
Fig. 2. RNAi of metacaspases in BSF *T. brucei*. (A). Western blot of cell extracts from an *MCA2-MCA3* RNAi clone (left panel) or an *MCA5* RNAi clone (right panel), incubated with (+) or without (–) tetracycline (tet) and probed with anti-MCA2-MCA3 or anti-MCA5 antibodies. Asterisk indicates crossreacting 48 kDa protein. (B) Upper panel, growth curve of an *MCA2-MCA3* and *MCA5* triple RNAi clone with or without induction with tetracycline. Lower panels, western blot of cell extracts from an *MCA2-MCA3* and *MCA5* triple RNAi clone, with or without induction with tetracycline, probed with anti-MCA2-MCA3 (left) or anti-MCA5 antibodies (right). (C) Upper panel, normal cell-cycle progression in wild-type BSF *T. brucei*. The kinetoplast division occurs before nuclear division, ultimately followed by cytokinesis. Images illustrate various cell stages with DAPI-stained nuclei (N) and kinetoplasts (K) (white); insets show kinetoplast at higher magnification (blue). Lower panels show nucleus and kinetoplast configurations with or without triple RNAi induction with tetracyline. Others, cells with an abnormal configuration but excluding 2N1K cells. For each time point, 200 cells were analysed. (D) Upper panel, analysis of kinetoplast configuration in 1N1K cells after induction with tetracycline. Bottom panels, aberrant cell-cycle progression in *MCA2-MCA3-MCA5* RNAi-induced BSF *T. brucei*. Images of representative triple RNAi-induced BSF *T. brucei*. Inset shows kinetoplast at higher magnification. Bars, 10 μm.
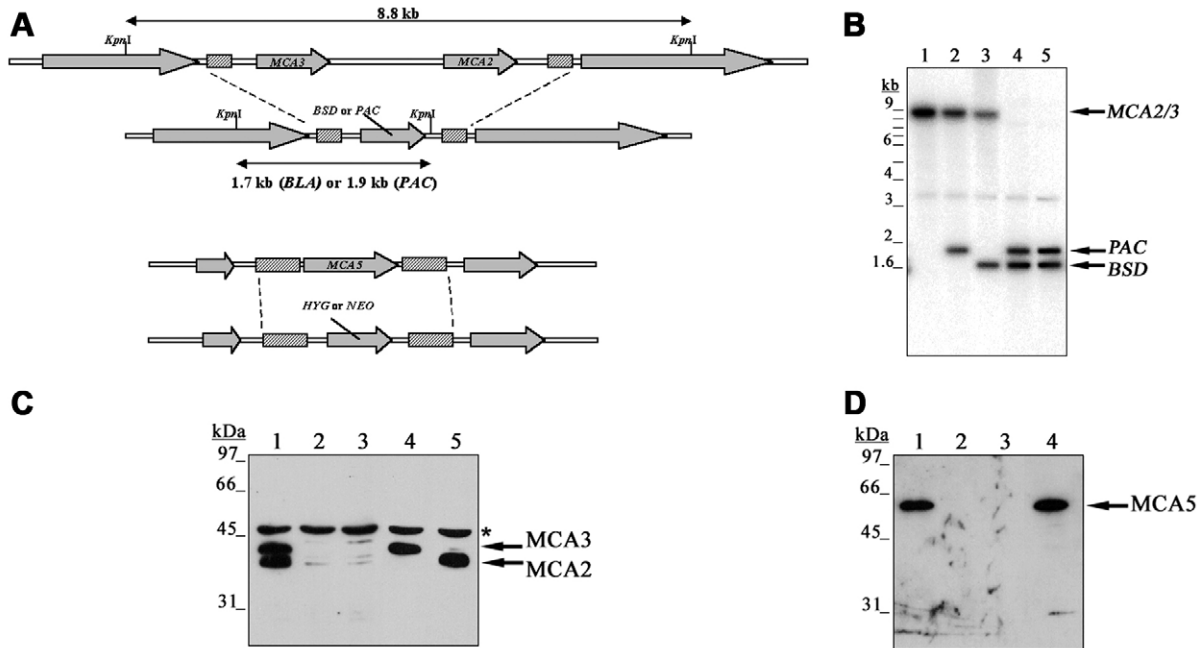
Fig. 3. Generation of metacaspase null mutants. (A) Schematic representation of the *MCA2-MCA3* and *MCA5* loci together with constructs for gene knockout. Open reading frames (ORFs) are shown as arrows, flanking DNA sequences for targeting are shown as boxes. The predicted fragment sizes of *Kpn*I-digested DNA for both native and modified *MCA2-MCA3* locus is shown. *BSD*, blasticidin-resistance gene; *PAC*, puromycin-resistance gene; *HYG,* hygromycin-resistance gene; *NEO,* neomycin-resistance gene. (B) Southern blot analysis of Δ*mca2/3*. Genomic DNA was digested with *Kpn*I, separated on a 1% agarose gel, blotted onto Hybond-P membrane and hybridised with a ^{32}P-labelled DNA probe comprising the 5′ flanking region used in the knockout strategy. Lane 1, wild type; lane 2, *PAC* heterozygote; lane 3, *BSD* heterozygote; lane 4, Δ*mca2/3* clone 1; lane 5, Δ*mca2/3* clone 2. (C) Total cell lysates were prepared from BSF parasites and 5×10^6 cell equivalents subjected to SDS-PAGE and transferred to PVDF membrane prior to immunoblotting with rabbit anti-MCA2-MCA3 antibodies. Lane 1, wild type; lane 2, Δ*mca2/3*; lane 3, Δ*mca2/3*Δ*mca5*; lane 4, Δ*mca2/3*Δ*mca5:MCA3*; lane 5, Δ*mca2/3*Δ*mca5:MCA2*. MCA2 and MCA3 are indicated. Asterisk indicates crossreacting 48 kDa protein. (D) Total cell lysates were prepared from BSF parasites and 5×10^6 cell equivalents subjected to SDS-PAGE and transferred to PVDF membrane prior to immunoblotting with sheep anti-MCA5 antiserum. Lane 1, wild type; lane 2, Δ*mca5*; lane 3, Δ*mca2/3*Δ*mca5*; lane 4, Δ*mca2/3*Δ*mca5:MCA5*. MCA5 is indicated.

of the RNAi data, it was predicted that triple null mutants could not be generated. However, independent Δ*mca2/3*Δ*mca5* clones were isolated. These clones initially displayed a significantly reduced growth rate compared with wild-type parasites, but after several weeks in culture the growth rate had returned to that of wild-type parasites. At early stages of selection the Δ*mca2/3*Δ*mca5* parasites also showed a higher number of cells at the pre-cytokinesis stage of the cell cycle than wild-type parasites (wild type: 71% 1N1K, 18% 1N2K, 9% 2N2K; Δ*mca2/3*Δ*mca5*: 54% 1N1K, 24% 1N2K, 17% 2N2K) suggesting a pre-cytokinesis cell-cycle block. Western blotting confirmed the absence of MCA2, MCA3 and MCA5 in the triple mutants (Fig. 3C,D). Re-expression of each *MCA* gene in Δ*mca2/3*Δ*mca5* parasites (e.g. Δ*mca2/3*Δ*mca5:MCA5*) was performed by targeting into the tubulin array and western blotting confirmed that expression of MCA2, MCA3 and MCA5 was similar to wild-type levels (Fig. 3C,D). After several weeks in culture, Δ*mca2/3*Δ*mca5* parasites had the same virulence to mice as wild-type and Δ*mca2/3* trypanosomes. These data show that in these clones, sequential deletion of MCA2, MCA3 and MCA5 did not affect the viability of BSF trypanosomes in culture or to mice. Thus, with BSF *T. brucei* there was a major difference in the consequences of knocking down MCA2, MCA3 and MCA5 expression in the RNAi cell lines, which was

lethal, and the sequential deletion of *MCA2*, *MCA3* and *MCA5*, which was not lethal.

To test whether the metacaspases are involved in prostaglandin D$_2$-induced cell death in BSF *T. brucei*, wild-type BSF parasites and the Δ*mca2/3*Δ*mca5* triple null mutants were treated with prostaglandin D$_2$ and their growth characteristics assessed. As previously reported, prostaglandin D$_2$ caused death (Figarella et al., 2005), but no difference in the kinetics of cell death was noticed between the two lines (not shown), demonstrating that MCA2, MCA3 and MCA5 are not required as effectors of prostaglandin D$_2$-induced cell death in BSF *T. brucei*. In addition, there was no processing of the three metacaspases, analysed by western blotting of BSF cell extracts, after treatment with prostaglandin D$_2$ for 8 and 24 hours (data not shown).

Metacaspases are located with RAB11 in recycling endosomes

The MCA5 antiserum was used for immunofluorescence studies. In BSF *T. brucei*, MCA5 localised to a well-defined sub-compartment of the cell located predominantly between the nucleus and kinetoplast (Fig. 4A-C). This is an area of the cell that contains the endosomes, lysosome and organelles of the secretory system (McConville et al., 2002; Overath and

Engstler, 2004). Since the antiserum raised against the peptide of MCA2 and MCA3 showed crossreactivity with other proteins, HA-epitope-tagged versions of MCA2 and MCA3 were generated and integrated at the tubulin locus in BSF parasites. Western blot analysis with an anti-HA monoclonal
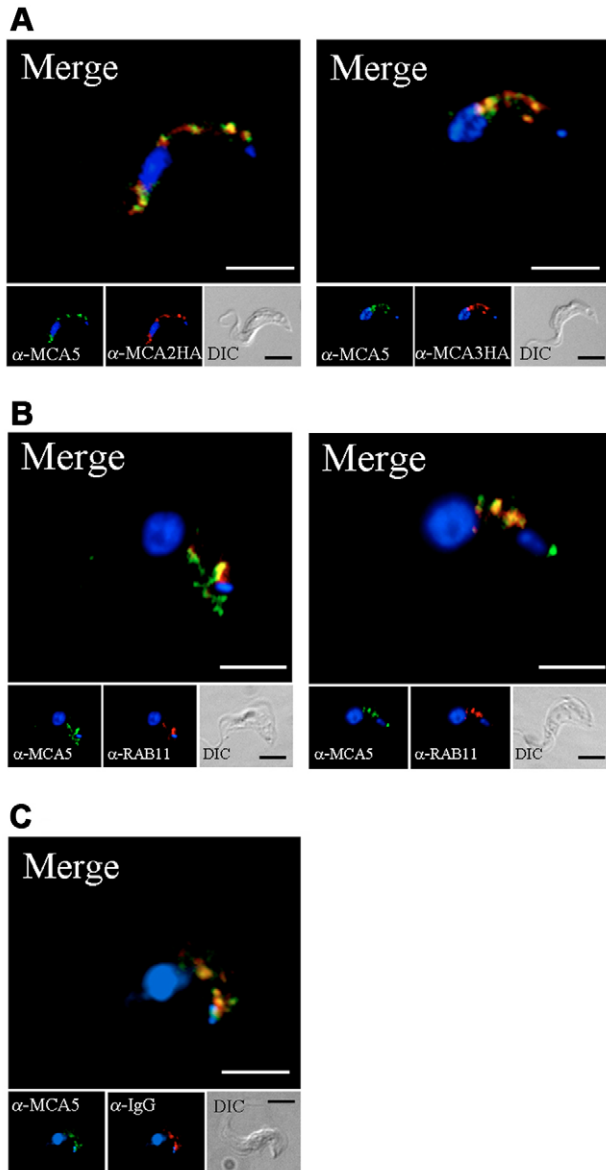

Fig. 4. Location of metacaspases. (A) BSF *T. brucei* parasites expressing either MCA2HA or MCA3HA proteins were fixed and co-stained with anti-HA monoclonal antibody (red) and sheep anti-MCA5 antiserum (green). (B) BSF parasites were fixed and stained with rabbit anti-RAB11 (red) and sheep anti-MCA5 antiserum (green). Single-slice images were analysed with volume deconvolution by using nearest-neighbour algorithm. (C) BSFs were incubated with rabbit anti-VSG221 antiserum at 4°C for 30 minutes and then returned to 37°C for 30 minutes. Fixed and permeabilised cells were stained with anti-MCA5 antiserum (green) and anti-rabbit IgG (red). For all images DNA was visualised with DAPI (blue). DIC images of the parasite are shown. Colocalisation is shown in yellow. Bars, 10 μm.

antibody confirmed that both MCA2HA and MCA3HA were expressed (Fig. 1C). Immunofluorescence revealed MCA2HA and MCA3HA to be localised to a compartment located between the nucleus and kinetoplast and had consistent morphology in all cells analysed (Fig. 4A). A high level of colocalisation was found between MCA5 and both MCA2HA as well as MCA3HA in BSF parasites, showing that the three metacaspases are associated with the same compartment.

To define the sub-cellular compartment in which the metacaspases are located, we carried out colocalisation studies with a variety of well-established organelle markers in BSF parasites (supplementary material Fig. S2). The early endosomes were selectively labelled at 4°C with a tomato-lectin FITC-conjugate (Jeffries et al., 2001), and cells were then co-stained with MCA5. There was clearly no colocalisation of the two signals, showing that the metacaspases are not located in early endosomes. Similarly, no colocalisation of MCA5 was found with lysotracker (Magez et al., 1997), or BODIPY-TR ceramide (Field et al., 2000). Although MCA5-positive structures were localised close to these organelles, the results show that metacaspases are not located in the lysosomal compartment or in the Golgi network.

Having ruled out metacaspase association with early endosomes, the lysosomal compartment and the Golgi network, an analysis of recycling endosomes was carried out with an antibody specific for RAB11, a small GTPase that is an established marker for this compartment in *T. brucei* (Jeffries et al., 2001; Grünfelder et al., 2003) and other eukaryotes (Volpicelli et al., 2002; Moore et al., 2004). Significant colocalisation of RAB11 and MCA5 was observed by using deconvolution fluorescence microscopy in BSF parasites (Fig. 4B), although separate localisation was also observed for both proteins. The colocalisation was further supported with immunogold transmission-electron-microscopy studies, which showed that RAB11 and MCA5 colocalised in distinct areas of the cell (Fig. 5). Colocalisation was found particularly between nucleus and kinetoplast and also surrounding the flagellar pocket (Fig. 5C). Although labile membrane structures were not easily visualised with our mild fixation procedures, an inferred peripheral pattern was in some cases observed for RAB11 labelling (e.g. Fig. 5A,B). Distinct localisation of both proteins, similar to that shown in the fluorescence studies, was evident from the three sites labelled in Fig. 5D. High-pressure freezing techniques and electron microscopy have shown that half of all endosomal cisternae are recycling endosomes that are RAB11-positive (Grünfelder et al., 2003). The RAB11 compartment in *T. brucei* has been shown to contain recycling receptors and their cargo, such as transferrin receptor and/or transferrin, and VSG and/or anti-VSG antibody (Jeffries et al., 2001). In this study, we found a significant level of colocalisation of internalised anti-VSG 221 antibody and MCA5 (Fig. 4C). These data provide evidence that a proportion of metacaspases of *T. brucei* are in close association with RAB11-positive recycling endosomes and their cargo.

Metacaspases are not required for efficient recycling of VSG or the degradation of anti-VSG antibodies

To establish whether the metacaspases are involved in the VSG recycling process in trypanosomes, wild-type parasites were compared with Δmca2/3Δmca5 and triple RNAi parasites. Surface VSG was biotinylated at 4°C prior to 5 minutes of
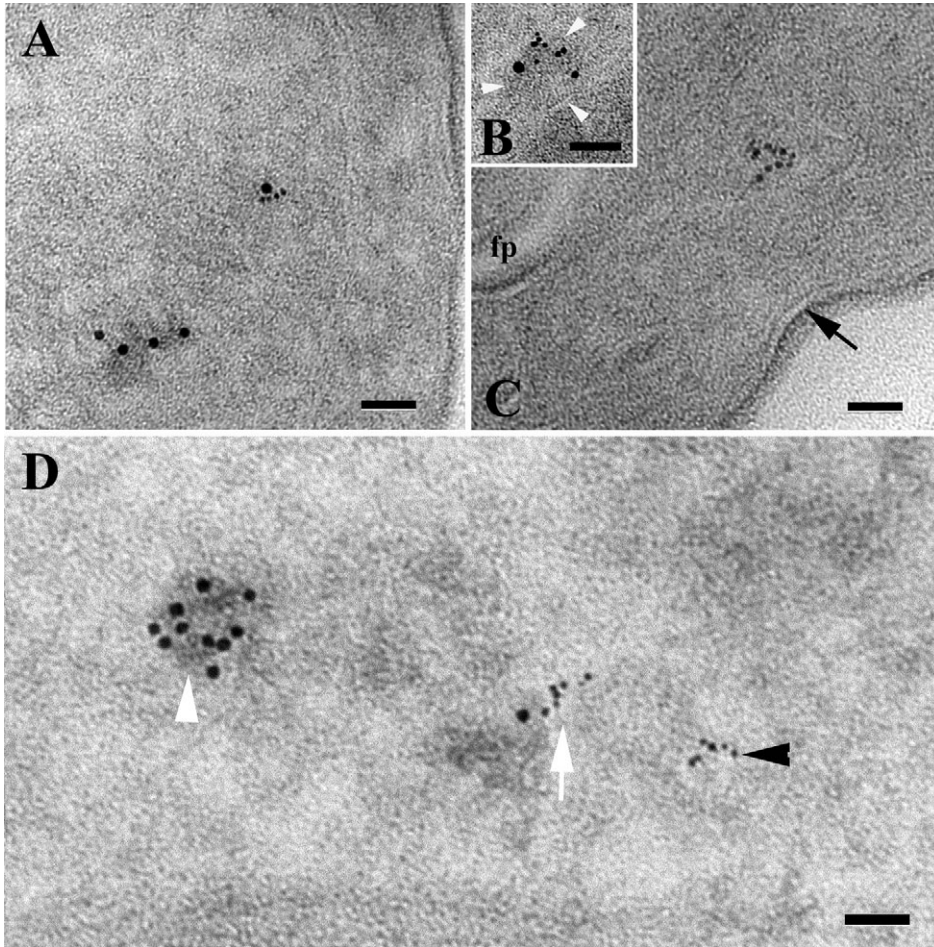
Fig. 5. Immunogold transmission-electron microscopy for BSF *T. brucei*. (A) Two vesicles labelled, one distinct MCA5 only (10 nm gold rabbit anti-sheep antibody) and one with RAB11 (6 nm gold goat anti-rabbit antibody) and MCA5. The particle groupings indicate an underlying bounding structure in the cytoplasm. (B) Presence of 10-nm and 6-nm gold particles at the periphery of a compartment. White arrowheads indicate bounding membrane. (C) Further example of RAB11 staining close to the flagellar pocket (D) Localisation of MCA5 only (white arrowhead), RAB11 with MCA5 (white arrow) and RAB11 only (black arrowhead) in *T. brucei*. Black arrow indicates surface coat; fp, flagellar pocket. Bars, 50 nm.

endocytosis at 37°C. Non-internalised biotin was cleaved from the parasite surface and cells were resuspended in medium for 0 to 10 minutes to allow time for recycling to occur. Immunofluorescence analysis of parasites showed that in both lines internalised biotin-VSG colocalised with RAB11-positive structures (data not shown) and that, following a 5-minute or 10-minute chase period, wild-type, Δ*mca2/3*Δ*mca5* and induced triple RNAi parasites were able to recycle this internalised VSG and return it to the cell surface (Fig. 6). It therefore appears that, the loss of MCA2, MCA3 and MCA5 does not prevent endocytosis of VSG, the trafficking through RAB11-positive vesicles or its subsequent return to the cell surface.

It has been documented previously that IgG-VSG immune complexes are internalised by *T. brucei* and that, while the VSG is recycled to the surface, the IgG is degraded intracellularly (O'Beirne et al., 1998; Jeffries et al., 2001; Pal et al., 2003). Anti-VSG IgG has been located in RAB11-positive vesicles, but the peptidases involved in the degradation of IgG and their location within the cell have not been identified. The finding that the metacaspases are present within recycling endosomes, which traffic anti-VSG IgG, raised the possibility that they might be involved in the degradation of the internalised IgG. To investigate this hypothesis, parasites were labelled with a polyclonal rabbit anti-VSG221 IgG at 4°C for 30 minutes, washed extensively and incubated at 37°C for a further 10 or 30 minutes. Following this period, parasites were

examined by fluorescence microscopy. The ability to internalise and degrade antibody was unimpaired in Δ*mca2/3*Δ*mca5* and the triple RNAi mutant eight hours after induction (Fig. 7A). Whole-cell lysates from wild type and Δ*mca2/3*Δ*mca5* (Fig. 7B), and TCA precipitations of the culture medium (Fig. 7C) were then subjected to SDS-PAGE, transferred to PVDF membrane and probed with an horseradish peroxidase (HRP)-conjugated anti-rabbit IgG to determine the fate of the internalised antibodies. Examination of cell-associated anti-VSG221 IgG illustrated that there was no build-up of IgG within Δ*mca2/3*Δ*mca5* parasites compared with wild-type parasites (Fig. 7B). A single protein, corresponding to rabbit heavy-chain IgG, was detected at equivalent levels in both cell lines. Analysis of the secreted products illustrated that the degradation of the anti-VSG IgG was very similar in Δ*mca2/3*Δ*mca5* parasites and wild-type parasites (Fig. 7C). These data show that the Δ*mca2/3*Δ*mca5* parasites are still functional with regard to anti-VSG antibody internalisation, degradation and secretion, and show that the absence of MCA2, MCA3 and MCA5 from recycling endosomes does not affect this process.

The *T. brucei* transferrin receptor is a low-abundance protein complex, encoded by two homologous genes *ESAG6* and *ESAG7* (Steverding et al., 1994; Salmon et al., 1994), limited in its distribution to the flagellar pocket (Steverding et al., 1994). Following internalisation of the receptor-transferrin complex, the reduction in pH within the endosomal system is

believed to cause dissociation of transferrin from the receptor (Dautry-Varsat et al., 1983; Maier and Steverding, 1996). The transferrin receptor is then recycled back to the flagellar pocket by Rab11-positive recycling endosomes (Jeffries et al., 2001) and degraded transferrin is secreted (Steverding et al., 1995; Pal et al., 2003). Analysis of wild-type and $\Delta mca2/3\Delta mca5$ parasites showed that both parasites were able to internalise and degrade transferrin (data not shown), showing that the proteolysis of transferrin was unaffected by loss of MCA2, MCA3 and MCA5.

Discussion

The *T. brucei* genome encodes five putative metacaspases (Szallies et al., 2002; Mottram et al., 2003). MCA1-MCA4 are predicted to have molecular masses of 38 to 40 kDa, whereas MCA5 has an additional C-terminal extension of approximately 15 kDa (Mottram et al., 2003). The *MCA5* gene of *T. brucei* and the single *MCA* of *L. major* are syntenic, and phylogenetic analysis suggests that the encoded proteins are more closely related to ScYCA1 than are MCA1-4 of *T. brucei* (data not shown). This suggests that MCA5 is the basal metacaspase and the possible progenitor of the other trypanosome MCA genes. This idea is also supported by the findings that in *T. brucei* MCA2 and MCA3 are BSF specific, whereas MCA5 is constitutive and expressed in both the mammalian BSF and in the insect PCF. The occurrence of multiple MCA proteins in *T. brucei*, with MCA2-MCA3 being only expressed in BSF, suggests that these enzymes play a role that relates closely to the parasite's survival in the bloodstream of a mammalian host. This study aimed to gain insight into what this is.

The detection of the three metacaspases apparently close to their full-length predicted masses in wild-type parasites cultured in vitro suggests that the metacaspases do not undergo any caspase-like large-scale processing events, at least under the growth conditions tested. A variety of stressful conditions, such as mild heat shock and mild osmotic shock, were tested with BSF trypanosomes in attempts to induce processing of the metacaspases, but none was detected. Likewise, no processing was detected in this study after treatment with the cell-death-inducing molecule prostaglandin D_2 (Figarella et al., 2005). Overexpression of the single metacaspase (YCA1) in yeast revealed apparent processing, which was absent when the putatively active site cysteine was substituted (Madeo et al., 2002). *Arabidopsis thaliana* has nine metacaspase genes, three of which were classified as type-I metacaspases, whereas the remaining six are type-II metacaspases (Uren et al., 2000; Vercammen et al., 2004). Expression of N-terminally tagged
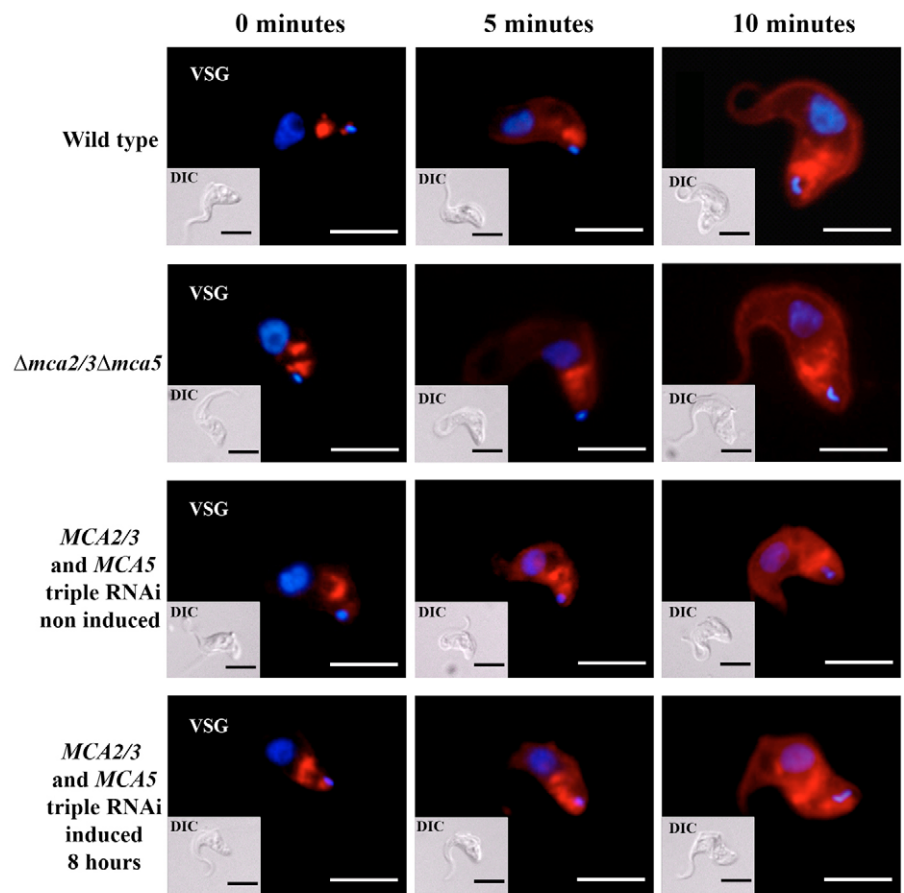

Fig. 6. Recycling of VSG. Wild-type, $\Delta mca2/3\Delta mca5$ and triple RNAi lines, with or without induction with tetracycline for 8 hours. Parasites were biotinylated at 4°C prior to incubation at 37°C for 5 minutes in HMI-9 medium. Remaining surface label was then cleaved by incubation with 50 mM glutathione at 4°C. Cells were prepared for fluorescence microscopy both immediately after the glutathione incubation and following a 5- or 10-minute chase period in HMI-9 medium at 37°C. Parasites were stained with Texas-Red-conjugated streptavidin (red). DNA was visualised with DAPI (blue). Insets, DIC images of the parasite. Bars, 10 μm.

type-II metacaspases in *Escherichia coli* showed that the enzymes undergo caspase-like autocatalytic processing, have arginine/lysine substrate specificity, but do not cleave caspase substrates (Vercammen et al., 2004). Thus, the failure to detect any caspase-like processing of the metacaspases of *T. brucei* in this study suggests that the *T. brucei* metacaspases are distinct from both that of yeast and the type-II metacaspases of plants. Indeed, the *T. brucei* metacaspases may well be more similar to the type-I plant metacaspases, which also did not display any processing under normal growth condition (Vercammen et al., 2004).

The genetic manipulation studies revealed an interesting difference between MCA downregulation with RNAi and MCA deletion with gene knockout. The $\Delta mca2/3\Delta mca5$ BSF clones grew very poorly during initial selection, yet recovered over several weeks to grow at the same rate as wild-type parasites. It seems that the parasites were able to adapt to the removal of first MCA2 and MCA3 and then MCA5, possibly by upregulating other peptidases or by activating alternative signalling pathways. RNAi, by contrast, led to rapid
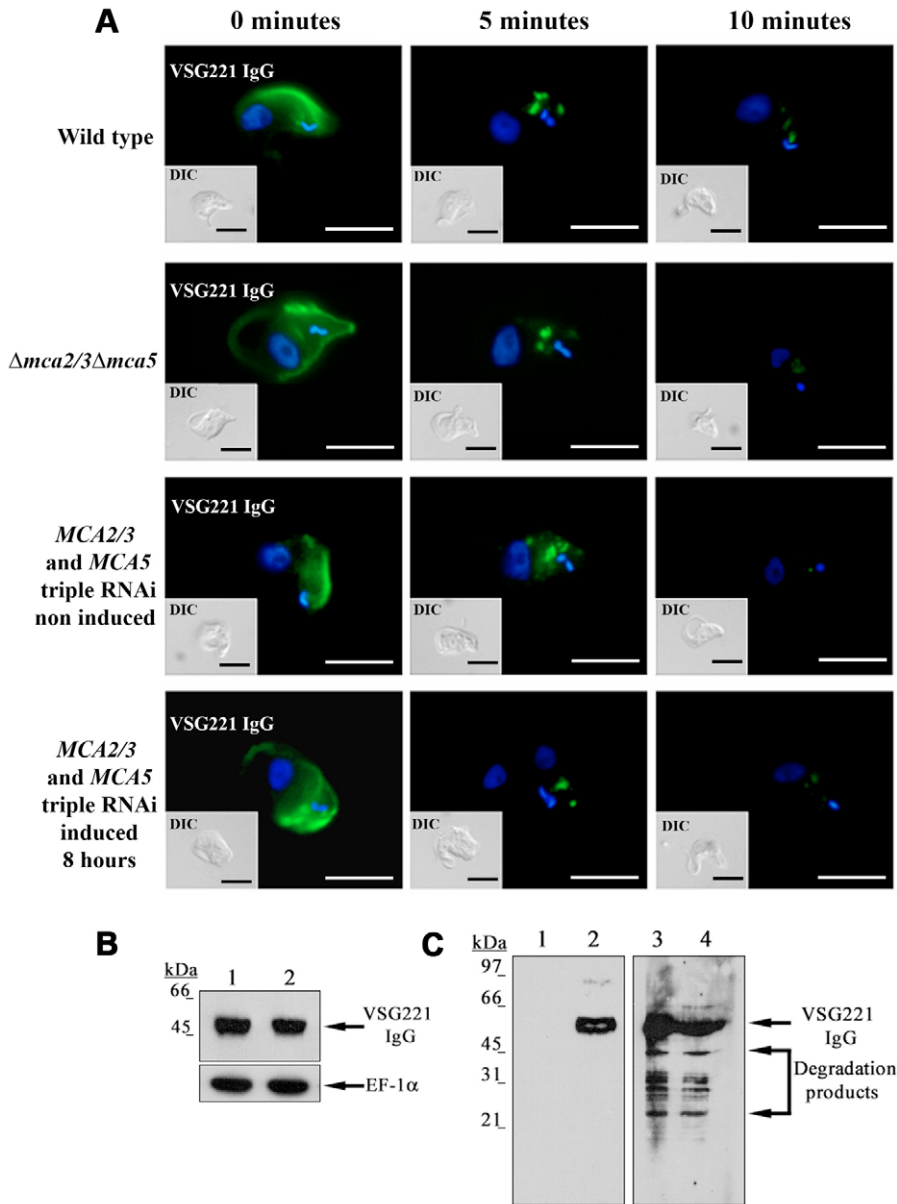
Fig. 7. Degradation of anti-VSG IgG. BSF wild-type, Δ*mca2/3*Δ*mca5* and triple RNAi lines, with or without induction with tetracycline for 8 hours. Parasites were labelled with anti-VSG221 IgG at 4°C in HMI-9 prior to incubation at 37°C for 5 and 10 minutes in HMI-9. (A) Parasites were fixed and stained with anti-rabbit-FITC conjugate (green) and DAPI (blue). Insets, DIC images of the parasite. Bars, 10 μm. (B) Whole-cell lysates were prepared after the 30-minute incubation and 5×10^6 cell equivalents subjected to SDS-PAGE and transferred to PVDF membrane prior to immunoblotting with an HRP-conjugated anti-rabbit IgG. Lane 1, wild-type BSF; lane 2, Δ*mca2/3*Δ*mca5*. EF-1α served as a loading control. (C) TCA precipitations of the culture medium were resuspended, subjected to SDS-PAGE and transferred to PVDF membrane prior to immunoblotting with an HRP-conjugated anti-rabbit IgG. Lane 1, without anti-VSG221 IgG; lane 2, with anti-VSG221 IgG in the absence of parasites; lane 3, wild-type BSF; lane 4, Δ*mca2/3*Δ*mca5* BSF. Anti-VSG221 IgGs are indicated together with degradation products.

downregulation of expression of all three genes at once. We postulate that it is the rapid removal of all three genes at once that resulted in the lethal effect, the parasite can not adapt to overcome this. The data suggest that, in BSF *T. brucei*, MCA2 and MCA3 can compensate for the lack of MCA5 and vice-versa, and this is supported by the finding that the three metacaspases are located in the same subcellular compartment.

Immunofluoresence and electron microscopy studies suggest that a significant proportion of MCA2, MCA3 and MCA5 are located in the same compartment as RAB11 (Fig. 4B and Fig. 5). RAB11 has multiple functions in mammalian cells, with a primary role in recycling endosomes (Ullrich et al., 1996) and the *trans*-Golgi network (Wilcke et al., 2000), although recent work also suggests an essential role for RAB11 in cytokinesis (Wilson et al., 2005). *T. brucei* RAB11 has been shown to be associated with recycling endosomes that traffic both VSG and the transferrin receptor in BSF (Jeffries et al., 2001; Grünfelder et al., 2003; Engstler et al., 2004). RAB11 is the only known stage-regulated RAB protein in *T. brucei*, displaying a much higher level of expression in the BSF compared with the PCF (Jeffries et al., 2001). Recent studies have shown that the total VSG surface coat is recycled very rapidly (within 12 minutes) (Engstler et al., 2004), thus the upregulated expression of RAB11 in the BSF correlates well with the increased requirement of recycling processes (Jeffries et al., 2001). The differential expression profile of MCA2 and MCA3 in *T. brucei*, together with the proteins' partial location in RAB11-positive vesicles, pointed towards the enzymes also being involved in recycling processes. As metacaspases are cysteine peptidases, our hypothesis was that the function involved essential processing of proteins within a RAB11-positive compartment. Thus, the findings that triple null mutants and triple RNAi mutants have no major defect in recycling of VSG or in degradation of anti-VSG antibodies is surprising. The phenotype of RAB11 RNAi and the triple MCA RNAi differ significantly. Although in both mutants

induction of RNAi leads to an immediate cessation of BSF growth, RAB11-induced RNAi cells become rounded with an enlarged flagellar pocket but show no specific cell-cycle block (Hall et al., 2005). By contrast, early after induction, triple MCA RNAi mutants display a delay in kinetoplast segregation and ultimately accumulate in a pre-cytokinesis cell-cycle state. At later time points, after MCA RNAi induction, cells accumulate with multiple nuclei and multiple kinetoplasts. This is because BSF parasites appear to lack a cell-cycle checkpoint that prevents additional rounds of S phase and mitosis prior to the completion of cytokinesis (Hammarton et al., 2003a). The precytokinesis block observed for triple MCA RNAi differs from that observed for RNAi of VSG, where a proposed VSG synthesis checkpoint prevents S phase re-initiation and cells accumulate with a 2N2K configuration (Sheader et al., 2005).

Together, these data argue against an involvement of metacaspases in RAB11-postive recycling endosomes but rather towards RAB11-positive endosomes involved in additional functions. In mammalian cells, RAB11-containing endosomes associate transiently with centrosomes to ultimately accumulate near the cleavage furrow, and are required for cytokinesis completion (Wilson et al., 2005). In PCF *T. brucei*, RAB11 was shown to migrate coordinately with the basal body during kinetoplast division (Jeffries et al., 2001). In this insect form of the parasite, the flagellar attachment zone area (the region that links the kinetoplast to the flagellum and is involved in kinetoplast division and/or segregation) of the new flagellum marks the position of the cleavage furrow during cytokinesis (Robinson et al., 1995; Kohl et al., 2003). Little is known about the process of cytokinesis in BSF trypanosomes, although it appears to differ significantly from mammalian cells (McKean, 2003; Hammarton et al., 2003b). Nevertheless, it is tempting to speculate that MCA2, MCA3 and MCA5 are involved in regulation of cleavage furrow formation during BSF cytokinesis.

How the trypanosome MCAs are directed to the compartments in which they reside is unclear. MCA3 and MCA5 have predicted signal peptides [SignalP 3.0 (http://www.cbs.dtu.dk/services/SignalP/) Sprob values: 0.929 for MCA3 and 0.986 for MCA5], whereas MCA2 does not. MCA3 and MCA5 are therefore likely to be sorted through the classic secretory pathway, whereas MCA2 might either be trafficked in association with MCA5, MCA3 or another ER-directed protein, or through an unconventional secretory pathway.

This study concentrated on MCA2, MCA3 and MCA5 of *T. brucei*. The genome of the parasite also encodes MCA1 and MCA4, although these proteins lack the predicted active site cysteine and so, presumably, are not active as cysteine peptidases. However, it cannot yet be ruled out that MCA1 or MCA4 might compensate for the lack of MCA2, MCA3 and MCA5, and fulfil their functions in the mutant parasites. Indeed it will be interesting to determine whether MCA1 or MCA4 are upregulated in the $\Delta mca2/3\Delta mca5$ line. MCA1 and MCA4 have extensive sequence identity with MCA2, MCA3 and MCA5, including the region within the catalytic centres (supplementary material Fig. S1), even though both proteins have substitutions at the predicted essential catalytic positions (Szallies et al., 2002; Mottram et al., 2003). Recent analysis has shown that inactive enzyme homologues are abundant in a variety of enzyme families, including peptidases (Pils and Schultz, 2004). It has been proposed that, by adapting existing protein modules, some of these 'dead' peptidases have evolved new regulatory functions. This could be the case for MCA1 and MCA4 of *T. brucei*. However, the loss of the key active-site-residues in these proteins, with the same residues being present in MCA2, MCA3 and MCA5, strongly suggest that the two sets of proteins have different functions.

Clearly, further analysis of the metacaspases in *T. brucei* is necessary to elucidate their roles and to provide insights into the regulatory networks to which both the active and dead MCAs contribute. Whether these might involve PCD-like phenomena is an open question. Although it has been proposed that metacaspases of yeast (Madeo et al., 2002; Herker et al., 2004; Wadskog et al., 2004) and plants (Hoeberichts et al., 2003; Bozhkov et al., 2004) have caspase-like functions associated with PCD, we have not been able to find any evidence for similar functions in BSF *T. brucei*. It cannot yet be ruled out that metacaspases are involved in apoptotic-like cell death in BSF *T. brucei*, however, the data available suggest that metacaspases have PCD-independent functions that could be associated within RAB11-positive endosomes. Metacaspases also occur in vesicles lacking RAB11, the significance of this awaits elucidation.

Materials and Methods
Culturing and transfection of parasites
Procyclic form (PCF) EATRO 795 *T. brucei* were cultured at 27°C in complete SDM79 medium (Brun and Schonenberger, 1979) supplemented with 10% (v/v) heat-inactivated foetal calf serum (FCS). Bloodstream form (BSF) 427 *T. brucei* were cultured at 37°C with 5% CO_2 in HMI-9 (Hirumi and Hirumi, 1989) supplemented with 10% (v/v) FCS and 10% (v/v) serum plus. Twenty micrograms of linearized DNA was used to transfect 5×10^7 mid-log-phase BSF parasites in 0.5 ml ZPFMG (132 mM NaCl, 8 mM Na_2HPO_4, 1.5 mM KH_2PO_4, 0.5 mM Mg acetate, 0.09 mM Ca acetate, 55 mM glucose, pH 7) in a 0.4-cm pulse-cuvette at 1.2 kV, 25 μF. After overnight recovery, selection of clones was achieved by limiting dilution with appropriate antibiotics (5 μg ml^{-1} blasticidin, 2.5 μg ml^{-1} puromycin, 5 μg ml^{-1} hygromycin, 1.25 μg ml^{-1} neomycin, 2.5 μg ml^{-1} phleomycin) in 24-well plates. For the RNAi study, the BSF 427 pLew13 pLew90-6 cell line was used (Wirtz et al., 1999). RNAi was induced with 1 μg ml^{-1} tetracycline when the cells were at a density of 1×10^5 cells ml^{-1}.

Plasmids
To generate the *MCA2-MCA3* RNAi construct, a 668 bp fragment, sharing 100% identity with *MCA2* and *MCA3*, was amplified by PCR from genomic DNA (strain 427) using Pfu polymerase (Stratagene) and the primer pair OL905 and OL906. The PCR product was cloned into the *Bam*HI and *Hin*dIII sites of p2T7^{ti} (LaCount et al., 2000) to generate pGL671. For the *MCA5* RNAi construct, a 416 bp fragment of *MCA5* was amplified by PCR from genomic DNA (strain 427) using Pfu polymerase and the primer pair OL944 and OL945. The PCR product was cloned into the *Bam*HI and *Hin*dIII sites of p2T7i to generate pGL714. For the triple *MCA2-MCA3-MCA5* RNAi construct, the 668bp *MCA2-MCA3* fragment was excised from pGL671 with *Hin*dIII and cloned into pGL714 pre-digested with *Hin*dIII to generate pGL905. pGL671, pGL714 and pGL905 were digested with *Not*I and gel-purified prior to transfection.

For deletion of the *MCA2* and *MCA3* locus, the 5′ flank of *MCA2* and the 3′ flank of *MCA3* were amplified by PCR using primer pairs OL969 and OL970, and OL971 and OL972, respectively, and cloned sequentially into the *Xba*I and *Apa*I sites flanking the *BSD* gene of pTBT-JBP KO (Cross et al., 2002) giving pGL802. Exchange of resistance genes was achieved by excising the *PAC* gene from pGL698 with *Eco*RI and cloning into the same sites present in pGL802, replacing the *BSD* gene with *PAC* and generating pGL808. pGL802 and pGL808 were digested with *Not*I-*Xho*I and the *PUR/BSD* containing fragments purified for transfection. Gene deletion was by homologous recombination, replacing the locus containing *MCA2* and *MCA3* and utilizing tubulin intergenic regions contained within pGL802 and pGL808 to ensure expression of drug resistance genes.

For deletion of *MCA5*, the 5′ and 3′ flanks of the gene were amplified by PCR using primer pairs OL1135 and OL1131, and OL1132 and OL1134, respectively, and cloned sequentially into the *Not*I-*Xba*I and *Apa*I sites flanking the *BSD* gene in pGL802. The *BSD* gene was then excised with *Eco*RI and replaced with both *HYG* and *NEO* resistance genes to generate pGL906 and pGL907. These were then

digested with *Not*I and *Eco*RV, and the fragments containing *HYG* or *NEO* purified for transfection.

For re-expression of *MCA2*, *MCA3* and *MCA5*, the ORFs were excised from pGL863, pGL864 and pGL805, respectively, with *Nde*I and *Xho*I, blunt-ended and cloned into pRM481 (a gift from Richard McCulloch, WCMP, University of Glasgow, UK), cut with *Eco*RV, to generate pGL867, pGL868 and pGL927. These plasmids were then digested with *Hind*III and *Xba*I, and purified for transfection.

To generate HA-tagged MCA2 and MCA3, equal molar concentrations of OL1225 and OL1226 were heated at 95°C for 10 minutes, allowed to cool slowly to room temperature and then ligated into *Bgl*II-*Xho*I digested pGL863 and pGL864 to generate pGL865 and pGL866, respectively. These modified genes were then excised with *Nde*I and *Xho*I, and inserted into pGL884 as described above, generating pGL878 and pGL879. Maps and sequence of all plasmids can be provided on request.

Primer sequences are follows OL905: 5′-AGGATCCATGGGTCGCGACACC-TCTTC-3′; OL906: 5′-GAAGCTTAGCGCCTGTAGAACCCGTACC-3′; OL944: 5′-GCGAATTCATGGACGCAGCTCTCGCTTTGC-3′; OL945: 5′-GCAAGCT-TACATCGTACACAAGCCATGCC-3′; OL969: 5′-AATCTAGAGCGGCCGCAA-GGGGTGACGAAACAGGAGC-3′; OL970: 5′-AATCTAGACTCATCCGCATA-TGTATTCG-3′; OL971: 5′-TTGGGCCCGTTTCTGCCCTTTGGTTCGC-3′; OL972: 5′-AAGGGCCCCTCGAGTTATGTCCAATAGCGGTGGC-3′; OL1131: 5′-AGTCTAGAGCTTCACCCTCTTTTCCCGAAC-3′; OL1132: 5′-ATGGGC-CCATGTCTATGACCCACCCTTCCC-3′; OL1134: 5′-ATGGGCCCGAATCAG-TCGGAAGTGGTCACATGACC-3′; OL1135: 5′-AAGCGGCCCGCATGTTTCG-TATCCGAGGGGTTGG-3′; OL1225: 5′-GATCCATCCAATACCCCTACGACGT-CCCGGACTATGCCTAGC-3′; OL1226: 5′-TCGAGCTAGGCATAGTCCGGGA-CGTCGTAGGGGTATTGGATG-3′. Table 1 in supplementary material describes the plasmids used in this study.

Antisera and immunoblotting

Antiserum specific to MCA2 and MCA3 was generated by immunization of a rabbit with an 80-mer peptide [NDVKQM…(69). …MDLPFT] (supplementary material Fig. S1). Immuno-purification of antiserum was performed with the peptide and antibodies stored in 50% (v/v) glycerol at –20°C. Antiserum specific to MCA5 was raised by immunization of a sheep with purified recombinant *T. brucei* MCA5. Anti-HA monoclonal antibodies were purchased from Roche, anti-EF-1α monoclonal antibodies were purchased from Upstate. Immuno-purified anti-Rab11 antibodies were a kind gift from Mark Field (Imperial College, London, UK) and anti-VSG221 antiserum was kindly provided by Mark Carrington (Department of Biochemistry, Cambridge University, UK).

T. brucei cell pellets were resuspended in Laemmli buffer, electrophoresed on 12% (w/v) SDS-PAGE gels and transferred onto PVDF membrane. Blocking was with either 5% (w/v) skimmed milk, or 1% (w/v) BSA in PBS [NaCl (0.15 M) and KHPO$_4$ (5 mM) pH 7.4], 0.05% Tween 20. Primary antibodies against MCA2, MCA3, MCA5, and EF-1α were used at dilutions of 1:10,000, antibodies against Rab11 and HA were used at 1:1000. HRP-conjugated anti-rabbit and anti-mouse IgG (Promega) and HRP-conjugated anti-sheep IgG (Santa Cruz) was used at 1:5000. Chemiluminescent detection was with the SuperSignal system (Pierce).

Immunofluorescence analysis

For immunofluorescence analyses, log-phase BSF parasites were washed in PBS and air-dried onto slides. Parasites were fixed in –20°C methanol for 15 minutes, whereupon permeabilisation was performed in –20°C acetone for 2 minutes. Slides were then blocked with either 5% (w/v) skimmed milk, or 1% (w/v) BSA in PBS with 0.05% Tween 20. Primary antibodies were used at the following dilutions: MCA5 antiserum at 1:1000, anti-HA antibodies at 1:500, anti-Rab11 at 1:200 in PBS, 0.05% Tween 20. Secondary conjugates used were: FITC-conjugated donkey anti-sheep IgG (Sigma) at 1:200, TRITC-conjugated rabbit anti-sheep IgG (Calbiochem) at 1:200, Texas Red-conjugated goat anti-rabbit IgG (Molecular Probes) at 1:200, and TRITC-conjugated goat anti-mouse IgG (Sigma) at 1:200 diluted in PBS, 0.05% Tween 20. Cells were viewed with a Zeiss UV microscope, and images were captured with an Orca-ER camera (Hamamatsu) and Openlab software version 3.0.4 (Improvision).

For microscopy, log-phase BSF parasites were washed in trypanosome dilution buffer (TDB; 20 mM Na$_2$PO$_4$, 2 mM NaH$_2$PO$_4$, 80 mM NaCl, 5 mM KCl, 1 mM MgSO$_4$, 20 mM glucose, pH 7.4), resuspended and fixed in 1% formaldehyde-TDB for 30 minutes at room temperature, then permeabilised with 0.1% Triton X-100 in TDB for 10 minutes and neutralised with 0.1 M glycine-TDB for 10 minutes. The parasites were then centrifuged 10 minutes at 300 *g*, resuspended in a small volume, spread on slides and air dried. Primary antibodies were used at the following dilutions: MCA5 antiserum at 1:250, anti-RAB11 antibodies at 1:250 in 0.1% Triton X-100 and 0.1% (w/v) BSA-PBS, and incubated with the cells for 2 hours at room temperature. Secondary conjugates used were: FITC-conjugated donkey anti-sheep IgG (Sigma) at 1:1000, Texas Red-conjugated goat anti-rabbit IgG (Molecular Probes) at 1:1000 in 0.1% Triton X-100 and 0.1% (w/v) BSA-PBS and incubated for 1 hour at room temperature. Cells were viewed as above. Deconvolution of single-slice images within stacks was carried out by using the ten nearest neighbours (Openlab software version 4.0.1 Improvision).

VSG recycling

Parasites were harvested at mid-log-phase and after three washes with ice-cold TDB, the cell density was adjusted to 1×10^8 cells ml^{-1} and the cells were incubated with 1 mM sulfo-NHS-SS-biotin (Pierce) for 10 minutes on ice. Tris-HCl (10 mM) pH 7.5 was added to stop the reaction. After three washes with of ice-cold TDB, parasites were re-suspended to a density of 1×10^7 ml^{-1} in pre-warmed HMI-9 and endocytosis allowed for 5 minutes at 37°C. Endocytosis was stopped and sulfo-NHS-SS-biotin removed from the cell surface by addition of ice-cold stripping-solution (HMI-9, 10% (v/v) FCS, 50 mM glutathione, pH 9) and a further 30 minutes incubation on ice. Parasites were subsequently washed a further three times in ice-cold TDB before returning them to HMI-9 at 37°C. Samples were taken at 5 and 10 minutes for analysis by western blot or immune fluorescence microscopy and processed as previously described. Biotin was detected using either Texas-Red-conjugated streptavidin (Molecular Probes) at 1:5000 or HRP-conjugated streptavidin (Sigma) at 1:10,000.

Anti-VSG221 antibody degradation

BSF parasites expressing VSG221 were harvested at mid-log-phase and labelled with anti-VSG221 antibodies at 4°C for 30 minutes in HMI-9 at a concentration of 1×10^7 parasites ml^{-1}. Parasites were then washed three times in ice cold serum-free HMI-9 and incubated, in pre-warmed, serum-free HMI-9, at 37°C for 10 or 30 minutes. Following this incubation period, samples were prepared for western blot or IFA as previously described. The culture medium following this period was also TCA-precipitated. One volume of a 0.5 mg ml^{-1} TCA solution was added to four volumes of culture medium, gently mixed and incubated on ice for 10 minutes. After centrifugation at 18,000 *g* for 5 minutes, the pellet was washed twice in ice cold acetone and briefly air-dried before re-suspension in 1× Laemmli sample buffer. Rabbit anti-VSG IgG was detected directly using HRP-conjugated anti-rabbit IgG (Promega).

Immuno-electron microscopy

Tokuyasu cryosectioning was performed on BSF *T. brucei* that had been chemically fixed in suspension for 5 minutes at room temperature, followed by 2 hours on ice in 2% paraformaldehyde and 0.1% glutaraldehyde in PBS (pH 7.2). After fixation, cells were rinsed in PBS, sedimented and embedded in 10% (w/v) gelatin in PBS. The gelatin-embedded cells were cut into blocks and rinsed in PBS, then infiltrated for 24 hours with 2.3 M sucrose in PBS. Specimen blocks were mounted on metal pins and frozen in liquid nitrogen before sectioning (70-80 nm) with a Leica Ultracut UCT/FCS. Sections were collected onto formvar-coated nickel grids and stored on ice-cold 2% (w/v) gelatin in PBS (Griffith and Posthuma, 2002).

Immuno-labelling of cryosections was performed at room temperature using standard procedures, with appropriate controls. Briefly, blocking was carried out using 0.1 M glycine for 20 minutes followed by 5% (w/v) BSA for 30 minutes; incubation with primary and secondary antibodies (gold conjugates) was for 1 hour. The incubation and washing buffer consisted of PBS (pH 7.4) with 0.2% BSA-c^{TM} (Aurion, The Netherlands). The MCA5 (1:500) and RAB11 (1:100) antibodies were detected with DASH-10 (1:20) and GAR-6 (1:20) gold conjugates (Aurion, Netherlands), respectively. Following labelling, the cryosections were contrast-stained with 2% (w/v) uranyl acetate in 0.15 M oxalic acid (pH 7.0) and embedded in 2% (w/v) methylcellulose with 0.1% uranyl acetate on platinum loops. Sections were viewed with a LEO 912 transmission electron microscope at 120 kV, digital images were prepared for presentation using Adobe Photoshop version 7.

References

Ameisen, J. C. (1996). The origin of programmed cell death. *Science* **272**, 1278-1279.

Ameisen, J. C., Idziorek, T., Billaut-Mulot, O., Loyens, M., Tissier, J.-P., Potentier, A. and Ouaissi, A. (1996). Apoptosis in a unicellular eukaryote (*Trypanosoma cruzi*): implications for the evolutionary origin and role of programmed cell death in the control of cell proliferation, differentiation and survival. *Cell Death Differ.* **2**, 285-300.

Arnoult, D., Akarid, K., Grodet, A., Petit, P. X., Estaquier, J. and Ameisen, J. C. (2002a). On the evolution of programmed cell death: apoptosis of the unicellular eukaryote *Leishmania major* involves cysteine proteinase activation and mitochondrion permeabilization. *Cell Death Differ.* **9**, 65-81.

Arnoult, D., Parone, P., Martinou, J. C., Antonsson, B., Estaquier, J. and Ameisen, J. C. (2002b). Mitochondrial release of apoptosis-inducing factor occurs downstream of cytochrome c release in response to several proapoptotic stimuli. *J. Cell Biol.* **159**, 923-929.

Barry, J. D. and McCulloch, R. (2001). Antigenic variation in trypanosomes: Enhanced phenotypic variation in a eukaryotic parasite. *Adv. Parasitol.* **49**, 1-70.

Bettiga, M., Calzari, L., Orlandi, I., Alberghina, L. and Vai, M. (2004). Involvement of the yeast metacaspase Yca1 in ubp10Δ-programmed cell death. *FEMS Yeast Res.* **5**, 141-147.

Bozhkov, P. V., Filonova, L. H., Suarez, M. F., Helmersson, A., Smertenko, A. P., Zhivotovsky, B. and von Arnold, S. (2004). VEIDase is a principal caspase-like activity involved in plant programmed cell death and essential for embryonic pattern formation. *Cell Death Differ.* **11**, 175-182.

Bozhkov, P. V., Suarez, M. F., Filonova, L. H., Daniel, G., Zamyatnin, A. A., Jr, Rodriguez-Nieto, S., Zhivotovsky, B. and Smertenko, A. (2005). Cysteine protease mcII-Pa executes programmed cell death during plant embryogenesis. *Proc. Natl. Acad. Sci. USA* **102**, 14463-14468.

Brun, R. and Schonenberger, M. (1979). Cultivation and *in vitro* cloning of procyclic forms of *Trypanosoma brucei* in a semi-defined medium. *Acta Trop.* **36**, 289-292.

Cross, M., Kieft, R., Sabatini, R., Dirks-Mulder, A., Chaves, I., and Borst, P. (2002). J-binding protein increases the level and retention of the unusual base J in trypanosome DNA. *Mol. Microbiol.* **46**, 37-47.

Das, M., Mukherjee, S. B. and Shaha, C. (2001). Hydrogen peroxide induces apoptosis-like death in *Leishmania donovani* promastigotes. *J. Cell Sci.* **114**, 2461-2469.

Dautry-Varsat, A., Ciechanover, A. and Lodish, H. F. (1983). pH and the recycling of transferrin during receptor-mediated endocytosis. *Proc. Natl. Acad. Sci. USA* **80**, 2258-2262.

Debrabant, A., Lee, N., Bertholet, S., Duncan, R. and Nakhasi, H. L. (2003). Programmed cell death in trypanosomatids and other unicellular organisms. *Int. J. Parasitol.* **33**, 257-267.

Engstler, M., Thilo, L., Weise, F., Grünfelder, C. G., Schwarz, H., Boshart, M. and Overath, P. (2004). Kinetics of endocytosis and recycling of the GPI-anchored variant surface glycoprotein in *Trypanosoma brucei*. *J. Cell Sci.* **117**, 1105-1115.

Ferguson, M. A. J. (1999). The structure, biosynthesis and functions of glycosylphosphatidylinositol anchors, and the contributions of trypanosome research. *J. Cell Sci.* **112**, 2799-2809.

Field, H., Sherwin, T., Smith, A. C., Gull, K. and Field, M. C. (2000). Cell-cycle and developmental regulation of TbRAB31 localisation, a GTP-locked Rab protein from *Trypanosoma brucei*. *Mol. Biochem. Parasitol.* **106**, 21-35.

Figarella, K., Rawer, M., Uzcategui, N. L., Kubata, B. K., Lauber, K., Madeo, F., Wesselborg, S. and Duszenko, M. (2005). Prostaglandin D2 induces programmed cell death in *Trypanosoma brucei* bloodstream form. *Cell Death Differ.* **12**, 335-346.

Griffith, J. M. and Posthuma, G. (2002). A reliable and convenient method to store ultrathin thawed cryosections prior to immunolabeling. *J. Histochem. Cytochem.* **50**, 57-62.

Grünfelder, C. G., Engstler, M., Weise, F., Schwarz, H., Stierhof, Y. D., Morgan, G. W., Field, M. C. and Overath, P. (2003). Endocytosis of a glycosylphosphatidylinositol-anchored protein via clathrin-coated vesicles, sorting by default in endosomes, and exocytosis via RAB11-positive carriers. *Mol. Biol. Cell* **14**, 2029-2040.

Hall, B. S., Smith, E., Langer, W., Jacobs, L. A., Goulding, D. and Field, M. C. (2005). Developmental variation in Rab11-dependent trafficking in *Trypanosoma brucei*. *Eukaryot. Cell* **4**, 971-980.

Hammarton, T. C., Clark, J., Douglas, F., Boshart, M. and Mottram, J. C. (2003a). Stage-specific differences in cell cycle control in *Trypanosoma brucei* revealed by RNA interference of a mitotic cyclin. *J. Biol. Chem.* **278**, 22877-22886.

Hammarton, T. C., Mottram, J. C. and Doerig, C. D. (2003b). The cell cycle of parasitic protozoa: potential for chemotherapeutic exploitation. *Prog. Cell Cycle Res.* **5**, 91-101.

Herker, E., Jungwirth, H., Lehmann, K. A., Maldener, C., Frohlich, K. U., Wissing, S., Buttner, S., Fehr, M., Sigrist, S. and Madeo, F. (2004). Chronological aging leads to apoptosis in yeast. *J. Cell Biol.* **164**, 501-507.

Hirumi, H. and Hirumi, K. (1989). Continuous cultivation of *Trypanosoma brucei* blood stream forms in a medium containing a low concentration of serum-protein without feeder cell-layers. *J. Parasitol.* **75**, 985-989.

Hoeberichts, F. A., Ten Have, A. and Woltering, E. J. (2003). A tomato metacaspase gene is upregulated during programmed cell death in *Botrytis cinerea*-infected leaves. *Planta* **217**, 517-522.

Holzmuller, P., Sereno, D., Cavaleyra, M., Mangot, I., Daulouede, S., Vincendeau, P. and Lemesre, J. L. (2002). Nitric oxide-mediated proteasome-dependent oligonucleosomal DNA fragmentation in *Leishmania amazonensis* amastigotes. *Infect. Immun.* **70**, 3727-3735.

Ivanovska, I. and Hardwick, J. M. (2005). Viruses activate a genetically conserved cell death pathway in a unicellular organism. *J. Cell Biol.* **170**, 391-399.

Jeffries, T. R., Morgan, G. W. and Field, M. C. (2001). A developmentally regulated Rab11 homologue in *Trypanosoma brucei* is involved in recycling processes. *J. Cell Sci.* **114**, 2617-2626.

Klemba, M. W. and Goldberg, D. E. (2002). Biological roles of proteases in parasitic protozoa. *Annu. Rev. Biochem.* **71**, 275-305.

Kohl, L., Robinson, D. and Bastin, P. (2003). Novel roles for the flagellum in cell morphogenesis and cytokinesis of trypanosomes. *EMBO J.* **22**, 5336-5346.

LaCount, D. J., Bruse, S., Hill, K. L., and Donelson, J. E. (2000). Double-stranded RNA interference in *Trypanosoma brucei* using head-to-head promoters. *Mol. Biochem. Parasitol.* **111**, 67-76.

Lee, N., Bertholet, S., Debrabant, A., Muller, J., Duncan, R. and Nakhasi, H. L. (2002). Programmed cell death in the unicellular protozoan parasite *Leishmania*. *Cell Death Differ.* **9**, 53-64.

Macias, M. J., Wiesner, S. and Sudol, M. (2002). WW and SH3 domains, two different scaffolds to recognize proline-rich ligands. *FEBS Lett.* **513**, 30-37.

Madeo, F., Herker, E., Maldener, C., Wissing, S., Lachelt, S., Herlan, M., Fehr, M., Lauber, K., Sigrist, S. J., Wesselborg, S. and Frohlich, K. U. (2002). A caspase-related protease regulates apoptosis in yeast. *Mol. Cell* **9**, 911-917.

Madeo, F., Herker, E., Wissing, S., Jungwirth, H., Eisenberg, T. and Frohlich, K. U. (2004). Apoptosis in yeast. *Curr. Opin. Microbiol.* **7**, 655-660.

Magez, S., Geuskens, M., Beschin, A., del Favero, H., Verschueren, H., Lucas, R., Pays, E. and De Baetselier, P. (1997). Specific uptake of tumor necrosis factor-alpha is involved in growth control of *Trypanosoma brucei*. *J. Cell Biol.* **137**, 715-727.

Maier, A. and Steverding, D. (1996). Low affinity of *Trypanosoma brucei* transferrin receptor to apotransferrin at pH 5 explains the fate of the ligand during endocytosis. *FEBS Lett.* **396**, 87-89.

Mazzoni, C., Herker, E., Palermo, V., Jungwirth, H., Eisenberg, T., Madeo, F. and Falcone, C. (2005). Yeast caspase 1 links messenger RNA stability to apoptosis in yeast. *EMBO Rep.* **6**, 1076-1081.

McConville, M. J., Mullin, K. A., Ilgoutz, S. C. and Teasdale, R. D. (2002). Secretory pathway of trypanosomatid parasites. *Microbiol. Mol. Biol. Rev.* **66**, 122-154.

McKean, P. G. (2003). Coordination of cell cycle and cytokinesis in *Trypanosoma brucei*. *Curr. Opin. Microbiol.* **6**, 600-607.

Moore, R. H., Millman, E. E., Alpizar-Foster, E., Dai, W. and Knoll, B. J. (2004). Rab11 regulates the recycling and lysosome targeting of beta2-adrenergic receptors. *J. Cell Sci.* **117**, 3107-3117.

Mottram, J. C., Helms, M. J., Coombs, G. H. and Sajid, M. (2003). Clan CD cysteine peptidases of parasitic protozoa. *Trends Parasitol.* **19**, 182-187.

Mottram, J. C., Coombs, G. H. and Alexander, J. (2004). Cysteine peptidases as virulence factors of *Leishmania*. *Curr. Opin. Microbiol.* **7**, 375-381.

Nguewa, P. A., Fuertes, M. A., Valladares, B., Alonso, C. and Perez, J. M. (2004). Programmed cell death in trypanosomatids: a way to maximize their biological fitness? *Trends Parasitol.* **20**, 375-380.

O'Beirne, C., Lowry, C. M. and Voorheis, H. P. (1998). Both IgM and IgG anti-VSG antibodies initiate a cycle of aggregation-disaggregation of bloodstream forms of *Trypanosoma brucei* without damage to the parasite. *Mol. Biochem. Parasitol.* **91**, 165-193.

Overath, P. and Engstler, M. (2004). Endocytosis, membrane recycling and sorting of GPI-anchored proteins: *Trypanosoma brucei* as a model system. *Mol. Microbiol.* **53**, 735-744.

Pal, A., Hall, B. S., Jeffries, T. R. and Field, M. C. (2003). Rab5 and Rab11 mediate transferrin and anti-variant surface glycoprotein antibody recycling in *Trypanosoma brucei*. *Biochem. J.* **374**, 443-451.

Pearson, T. W., Beecroft, R. P., Welburn, S. C., Ruepp, S., Roditi, I., Hwa, K. Y., Englund, P. T., Wells, C. W. and Murphy, N. B. (2000). The major cell surface glycoprotein procyclin is a receptor for induction of a novel form of cell death in African trypanosomes in vitro. *Mol. Biochem. Parasitol.* **111**, 333-349.

Pils, B. and Schultz, J. (2004). Inactive enzyme-homologues find new function in regulatory processes. *J. Mol. Biol.* **340**, 399-404.

Rawlings, N. D., Tolle, D. P. and Barrett, A. J. (2004). MEROPS: the peptidase database. *Nucleic Acids Res.* **32**, D160-D164.

Ridgley, E. L., Xiong, Z. H. and Ruben, L. (1999). Reactive oxygen species activate a Ca2+-dependent cell death pathway in the unicellular organism *Trypanosoma brucei*. *Biochem. J.* **340**, 33-40.

Robinson, D. R., Sherwin, T., Ploubidou, A., Byard, E. H. and Gull, K. (1995). Microtubule polarity and dynamics in the control of organelle positioning, segregation, and cytokinesis in the trypanosome cell cycle. *J. Cell Biol.* **128**, 1163-1172.

Salmon, D., Geuskens, M., Hanocq, F., Hanocq-Quertier, J., Nolan, D., Ruben, L. and Pays, E. (1994). A novel heterodimeric transferrin receptor encoded by a pair of VSG expression site-associated genes in *T. brucei*. *Cell* **78**, 75-86.

Sen, N., Das, B. B., Ganguly, A., Mukherjee, T., Tripathi, G., Bandyopadhyay, S., Rakshit, S., Sen, T. and Majumder, H. K. (2004). Camptothecin induced mitochondrial dysfunction leading to programmed cell death in unicellular hemoflagellate *Leishmania donovani*. *Cell Death Differ.* **11**, 924-936.

Seyfang, A., Mecke, D. and Duszenko, M. (1990). Degradation, recycling, and shedding of *Trypanosoma brucei* variant surface glycoprotein. *J. Protozool.* **37**, 546-552.

Sheader, K., Vaughan, S., Minchin, J., Hughes, K., Gull, K. and Rudenko, G. (2005). Variant surface glycoprotein RNA interference triggers a precytokinesis cell cycle arrest in African trypanosomes. *Proc. Natl. Acad. Sci. USA* **102**, 8716-8721.

Steverding, D., Stierhof, Y.-D., Chaudhri, M., Ligtenberg, M., Schell, D., Beck-Sickinger, A. G. and Overath, P. (1994). ESAG 6 and 7 products of *Trypanosoma brucei* form a transferrin binding protein complex. *Eur. J. Cell Biol.* **64**, 78-87.

Steverding, D., Stierhof, Y. D., Fuchs, H., Tauber, R. and Overath, P. (1995). Transferrin-binding protein complex is the receptor for transferrin uptake in *Trypanosoma brucei*. *J. Cell Biol.* **131**, 1173-1182.

Suarez, M. F., Filonova, L. H., Smertenko, A., Savenkov, E. I., Clapham, D. H., von Arnold, S., Zhivotovsky, B. and Bozhkov, P. V. (2004). Metacaspase-dependent programmed cell death is essential for plant embryogenesis. *Curr. Biol.* **14**, R339-R340.

Sudol, M. and Hunter, T. (2000). NeW wrinkles for an old domain. *Cell* **103**, 1001-1004.

Szallies, A., Kubata, B. K. and Duszenko, M. (2002). A metacaspase of *Trypanosoma brucei* causes loss of respiration competence and clonal death in the yeast *Saccharomyces cerevisiae*. *FEBS Lett.* **517**, 144-150.

Ullrich, O., Reinsch, S., Urbe, S., Zerial, M. and Parton, R. G. (1996). Rab11 regulates recycling through the pericentriolar recycling endosome. *J. Cell Biol.* **135**, 913-924.

Uren, G. A., O'Rourke, K., Aravind, L., Pisabarro, T. M., Seshagiri, S., Koonin, V.

E. and Dixit, M. V. (2000). Identification of paracaspases and metacaspases: two ancient families of caspase-like proteins, one of which plays a key role in MALT lymphoma. *Mol. Cell* **6**, 961-967.

Vercammen, D., van de Cotte, B., De Jaeger, G., Eeckhout, D., Casteels, P., Vandepoele, K., Vandenberghe, I., Van Beeumen, J., Inze, D. and Van Breusegem, F. (2004). Type II metacaspases Atmc4 and Atmc9 of *Arabidopsis thaliana* cleave substrates after Arginine and Lysine. *J. Biol. Chem.* **279**, 45329-45336.

Volpicelli, L. A., Lah, J. J., Fang, G., Goldenring, J. R. and Levey, A. I. (2002). Rab11a and myosin Vb regulate recycling of the M4 muscarinic acetylcholine receptor. *J. Neurosci.* **22**, 9776-9784.

Wadskog, I., Maldener, C., Proksch, A., Madeo, F. and Adler, L. (2004). Yeast lacking the SRO7/SOP1-encoded tumor suppressor homologue show increased susceptibility to apoptosis-like cell death on exposure to NaCl stress. *Mol. Biol. Cell* **15**, 1436-1444.

Weinberger, M., Ramachandran, L., Feng, L., Sharma, K., Sun, X., Marchetti, M., Huberman, J. A. and Burhans, W. C. (2005). Apoptosis in budding yeast caused by defects in initiation of DNA replication. *J. Cell Sci.* **118**, 3543-3553.

Welburn, S. C. and Murphy, N. B. (1998). Prohibitin and RACK homologues are up-regulated in trypanosomes induced to undergo apoptosis and in naturally occurring terminally differentiated forms. *Cell Death Differ.* **5**, 615-622.

Welburn, S. C., Dale, C., Ellis, D., Beecroft, R. and Pearson, T. W. (1996). Apoptosis in procyclic *Trypanosoma brucei rhodesiense in vitro*. *Cell Death Differ.* **3**, 229-236.

Wilcke, M., Johannes, L., Galli, T., Mayau, V., Goud, B. and Salamero, J. (2000). Rab11 regulates the compartmentalization of early endosomes required for efficient transport from early endosomes to the trans-golgi network. *J. Cell Biol.* **151**, 1207-1220.

Wilson, G. M., Fielding, A. B., Simon, G. C., Yu, X., Andrews, P. D., Hames, R. S., Frey, A. M., Peden, A. A., Gould, G. W. and Prekeris, R. (2005). The FIP3-Rab11 protein complex regulates recycling endosome targeting to the cleavage furrow during late cytokinesis. *Mol. Biol. Cell* **16**, 849-860.

Wirtz, E., Leal, S., Ochatt, C. and Cross, G. A. (1999). A tightly regulated inducible expression system for conditional gene knock-outs and dominant-negative genetics in *Trypanosoma brucei*. *Mol. Biochem. Parasitol.* **99**, 89-101.

Zangger, H., Mottram, J. C. and Fasel, N. (2002). Cell death in *Leishmania* induced by stress and differentiation: Programmed cell death or necrosis? *Cell Death Differ.* **9**, 1126-1139.